Initial Clinical Experience Imaging Scatterer Size and Strain in Thyroid Nodules

Thaddeus Wilson, PhD, Quan Chen, PhD, James A. Zagzebski, PhD, Tomy Varghese, PhD, Lester VanMiddlesworth, MD, PhD

Objective. This article describes a new research ultrasound scanner that can be programmed to produce elastograms and backscatter parametric images in real time. Its performance was evaluated in a clinical setting. ***Methods.*** Radio frequency data were acquired from 13 patients with thyroid nodules and from 4 normal thyroids, along with reference phantom data. Scatterer size was deduced by measuring the backscatter versus frequency and fitting data to a model. Strain was obtained by a cross-correlation method, comparing precompression and postcompression radio frequency signals. Scatterer size contrast was defined as the observed contrast between the "normal" and "abnormal" tissue in the same gland or, when considering diffuse conditions, by comparing with normal values. Strain contrast was estimated if abnormal and normal tissue was captured in the same palpation, that is, excluding diffuse disease, which was the case for 9 subjects. ***Results.*** On scatterer size images, 4 nodules exhibited positive contrast versus the adjacent normal parenchyma, indicating larger scatterers. Five nodules were isoechoic, and 4 had negative contrast. Four nodules exhibited positive strain contrast, indicating that they were softer than the normal parenchyma. Two nodules had the same brightness, and 3 were darker than the background thyroid tissue on strain images. ***Conclusions.*** Contrast was observed between nodules and thyroid parenchymal tissue for both types of parametric images. Further work is needed to determine whether the diagnostic importance of these parameters in characterizing thyroid nodules might be worthwhile. Both modes must be of a sufficient frame rate to provide real-time feedback to operators, which will require further work. ***Key words:*** acoustic backscatter coefficient; elastography; frequency-dependent backscatter; quantitative imaging; sonographic tissue characterization; thyroid.

Abbreviations
FNA, fine-needle aspiration; RF, radio frequency; TSH, thyrotropin

Received March 13, 2006, from the Department of Radiology, University of Tennessee, Memphis, Tennessee USA (T.W., L.V.); and Department of Medical Physics, University of Wisconsin-Madison, Madison, Wisconsin USA (Q.C., J.A.Z., T.V.). Revision requested March 22, 2006. Revised manuscript accepted for publication May 3, 2006.

This work was funded in part through National Institutes of Health grant R21CA100989-01A1.

Address correspondence to Thaddeus Wilson, PhD, Department of Radiology, University of Tennessee, 865 Jefferson Ave, Memphis, TN 38163 USA.

E-mail: tawilson@utmem.edu

Thyroid cancer accounts for an estimated 14,000 new cancer cases and more than 1000 deaths in the United States each year. The annual incidence is about 4 per 100,000 of the population. According to the *Guide to Clinical Preventive Services*, Second Edition,[1] the common form of screening for thyroid abnormalities, neck palpation, lacks the sensitivity (33%) for detecting cancer, and the false-positive rate with sonography is too large to avoid invasive tests, such as biopsy, to rule out cancer. However, both the 5- and 7-year survival rates among thyroid cancers show notable improvement with early diagnosis. Thus, the overall aim of this work was to develop methods for noninvasively diagnosing cancer in the thyroid earlier and more accurately than currently used diagnostic tests.

Most thyroid nodules are discovered by palpation. Most are benign, and the clinical challenge is to pick out those nodules that are malignant and require surgical excision. Patients in whom the nodule is hard or those in whom the nodule is attached firmly to surrounding tissues are thought to be at an increased risk of malignancy.[2] Further noninvasive evaluation may be done by measuring serum thyrotropin (TSH) levels, radioisotope scanning, and sonographic imaging. However, these tests are usually not specific enough to rule out cancer, although abnormal thyroid function may make it less likely. Thyrotropin levels, for example, are indicative of an abnormality in the pituitary gland. The production of TSH is controlled by the thyroid gland, which has a higher likelihood of being the cause of an abnormal value. High or low levels of TSH are clinically important and could be due to a cancer; however, further testing is required. In fact, high TSH levels even have the potential of acting as a promoter of cancer growth. Nuclear medicine scanning is used to classify suspected nodules as cold, warm, or hot. Malignancies are most closely associated with "cold nodules" on radioisotope scans; however, only 5% to 15% of cold nodules actually are malignant, so this classification is also associated with a high false-positive rate.

There is much interest in applying high-frequency gray scale sonographic imaging and Doppler methods to diagnose thyroid nodules. One use of sonography is to localize nodules for guidance of fine-needle aspiration (FNA) biopsy. It is generally accepted that sonography can assist in determining whether a nodule is confined to the thyroid or is outside the organ. It can also pinpoint the nodule location and internal regions for biopsy guidance. In addition, it can show whether a nodule is solid or cystic.[2] The ability to use sonography to classify nodules and distinguish whether they are benign or malignant is much more controversial, however. Features such as relative echogenicity, presence and appearance (fine or coarse) of calcifications, blood flow patterns and whether they are peripheral or internal, definition of nodule margins, through-transmission characteristics, and presence or absence of a sonographic "halo" circumscribing the nodule all are used in different classification schemes.[3] The sonographic appearance of the most common thyroid malignancy, papillary carcinoma, for example, includes hypoechogenicity (associated with a closely packed nodular cell content), microcalcifications, and hypervascularity.[3] Not all these signs are present in every case, and currently, no single sonographic feature is associated consistently with a nodule's being benign or malignant. Thus, in most centers, sonography remains an adjunct modality for detection, localization, and follow-up studies of thyroid masses.[4]

Fine-needle aspiration biopsy is the most widely used technique for detecting whether a thyroid nodule is malignant. Sensitivities exceeding 95% for classifying nodules have been reported. The success of the technique can, however, be highly variable, depending on the skill of the practitioner and the availability of an experienced cytologist. Thus, reported FNA sensitivities actually range widely, from 65% to 98%, and specificities range from 72% to 100%.[2]

Although FNA is a very useful technique for classifying thyroid nodules, the variable sensitivity among centers and a desire for better selection of patients subjected to needle biopsy continues to raise interest in developing more accurate imaging methods to detect thyroid cancers. Conventional sonographic imaging detects and displays only the amplitude of detected echoes. We think that there is considerably more information available in the frequency content of ultrasonic signals and the local strain distribution under compression. However, this information cannot be easily extracted even in most "high-end," state-of-the-art ultrasound scanners because they continue to provide only amplitude processing of the echo signals. Because the thyroid is very accessible to ultrasound, particularly for transducers operating at high frequencies and having extremely wide frequency bandwidths, this is an excellent clinical area to explore the usefulness of echo signal processing tools that researchers have found useful in areas such as the eye and kidney to generate data and images based on changes in the underlying tissue microstructure such as scatterer size and concentration.[5,6] These researchers operate as do we under the premise that different tissue abnormalities lead to variations that might be sensitive to quantitative imaging such as scatterer size. The thyroid is also easily palpated, which allows for generation of elastograms using freehand techniques similar to those being explored in the breast for differentiation of cancer.[7–9]

The purpose of this article is to present initial findings using a new research ultrasound scanner to image the thyroid. We programmed the machine to produce elastograms and backscatter parametric images in real time, albeit at slow frame rates. Here we present examples of its use by imaging thyroids of patients with nodules.

Materials and Methods

Patients

Data were acquired on an institutionally approved protocol following informed consent from 13 patients with suspected thyroid nodules or diffuse disease and from a normal group of 4 subjects. The study group included 10 women and 3 men with ages ranging from 21 to 76 years, with a mean of 46 years. Strain images were only acquired for 9 patients because some of the patients had a diffuse condition or simply had no nodule present. When determining relative contrast for scatterer size images in cases with diffuse disease, comparisons were made with scatterer sizes derived from the normal group. No children were imaged in this preliminary work.

Ultrasound Scanner

Thyroid nodules were scanned in vivo with an Ultrasonix ES500RP real-time scanner (Ultrasonix Medical Corporation, Bothell, WA) equipped with an L12-5 linear array transducer with an 8.25-MHz center frequency and an approximate 88% –6-dB bandwidth. To acquire radio frequency (RF) data, we used the Ultrasound Research Interface supplied by the manufacturer and developed a client program for real-time elastographic imaging to communicate with the Ultrasonix Ultrasound Research Interface and software server to acquire the RF data during the palpation procedure. Echo signals are digitized by the machine at a sampling rate of 40 MHz. Radio frequency signals are obtained from all beam lines in the frame up to an image depth of 7.8 cm, which has since been extended to a full frame acquisition on the company's newer scanner, the Sonix RP.

One of the thyroid nodules was scanned using a Terason Ultrasound (Burlington, MA) real-time portable scanner equipped with an 8-MHz linear array transducer with an approximate 60% bandwidth. To acquire RF data, we used a licensed application supplied by the manufacturer to extract the RF signals from a raw data file generated on the scanner for every acquisition. These signals were analyzed off-line. Data were acquired in a cine loop similar to the Ultrasonix system during freehand palpation. Echo signals are currently digitized at a rate of 40 MHz and can be obtained from all beam lines in the frame.

With either machine, both longitudinal and transverse scans were done by placing the probe directly in contact with the external neck wall over the site of the palpated nodule. Overall gain and time-gain compensation settings were optimized for gray scale images. For RF data collection, loops of echo data were acquired and then analyzed off-line. For elasticity imaging, the transducer was gently displaced back and forth at a slow (3-second period) rate as data were collected.

Scatterer Size Imaging

A method of measuring scatterer sizes using the frequency dependence of backscatter has been implemented in the University of Wisconsin-Madison laboratories.[10] Basically, the technique measures the backscatter coefficient versus frequency for the sample using a reference phantom method.[11] Then it compares backscatter versus frequency over the measurement bandwidth to model backscatter-versus-frequency curves, where each curve represents modeled data for a different-sized scatterer. The modeled scatterer size that yields the best fit to the measurement result is used to represent an effective scatterer size for the sample.[10] The reference phantom method enables correct backscatter-versus-frequency data for any location in the sonographically imaged field, facilitating use of this method for imaging. For the data from the Ultrasonix machine, the processing was carried out on the machine itself. However, for the Terason machine, only off-line processing was available. The reference phantom used had a nominal attenuation coefficient of 0.5 $dB \cdot cm^{-1} \cdot MHz^{-1}$, which is lower than that of the thyroid from other reported values higher than 1 $dB \cdot cm^{-1} \cdot MHz^{-1}$.[12] Attenuation corrections were, however, not implemented at this time.

Strain Imaging

Real-time elastographic images were constructed by following the well-established algorithms used for off-line elastography in our laboratories.[13] We acquired RF data for successive image pairs, saved these image buffers in system mem-

ory, and then applied a 1-dimensional normalized cross-correlation algorithm to compute frame-to-frame tissue displacements. A 3-microsecond window with 50% overlap was applied to the RF data in this analysis. From the tissue displacement data, a 3-point gradient operator was used to compute the local tissue strain. A 5-point median filter was then applied to reduce noise in the strain data matrix, which is then displayed as an image.

Results

Figure 1 was generated with data collected on the Terason portable laptop scanner. Figure 1A is a standard B-mode image frame of a solitary isoechoic nodule in the right lobe of an elderly female patient. The RF data from this frame, along with the RF data from the immediately subsequent image frame, was used to generate the elastogram in Figure 1B. The brightness on the elastogram indicates greater strain induced by the transducer compression, where percent strain is shown in the color bar. As described above, the elastographic processing uses a cross-correlation algorithm to measure time shifts in the echo data from one image frame to the next. In this case, the time shifts result from the sonographer-induced compression of the transducer during acquisition of the 60-frame series. The axial gradient of the measured time shift yields the elastogram. Figure 2 is a B-mode image of the same nodule taken from a slightly different orientation. It is included to illustrate the nodule margins (arrows) because the margins in Figure 1A are not easily delineated from the thyroid parenchyma. Interestingly, the corresponding elastogram has a notable difference in contrast versus the background in the area of the nodule. Notice that the nodule is difficult to perceive in the B-mode images, but it is easily identified in the elastogram. The biopsy sample contained follicular cells, macrophages, and other colloid consistent with benign multinodular goiter. The bright appearance of the nodule versus the background indicates that it is actually softer than the surrounding thyroid tissue. This finding is unlike results being reported for the breast, where the nodules often appear dark or stiffer than the adjacent parenchyma in the breast.

Figure 1. A, B-mode image obtained from a solid nodule in the thyroid with a Terason 8L4 portable laptop scanner. Arrows denote the proximal margins of the nodule. The nodule is isoechoic, and the margins are poorly delineated distally. **B**, The strain image has better margin delineation and indicates that the nodule has more strain, that is, is softer (brighter) under freehand compression than the adjacent parenchyma.

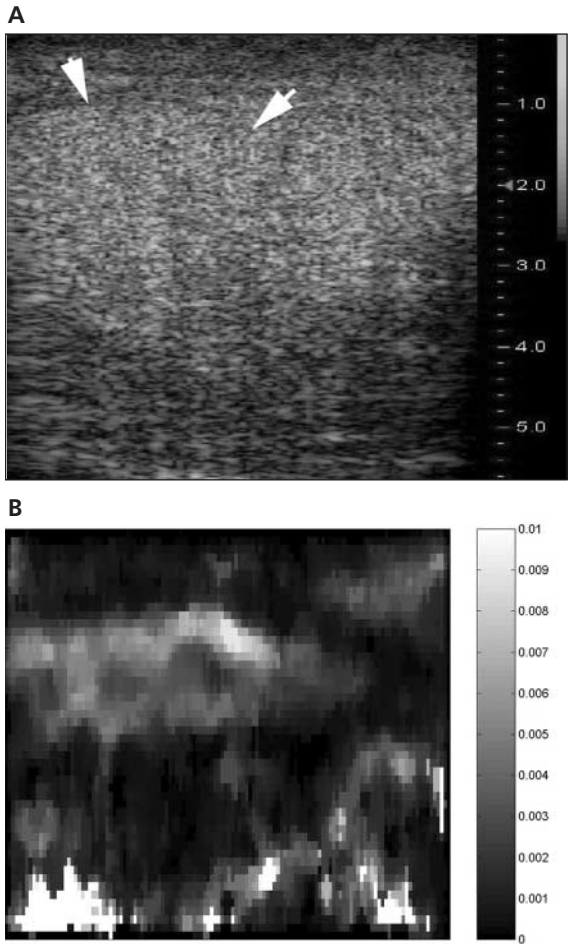

Figure 2. B-mode image obtained on the Terason scanner of the same lesion depicted in Figure 1 but with a slightly different orientation, allowing for better visualization of the margins (arrows) in this image format.

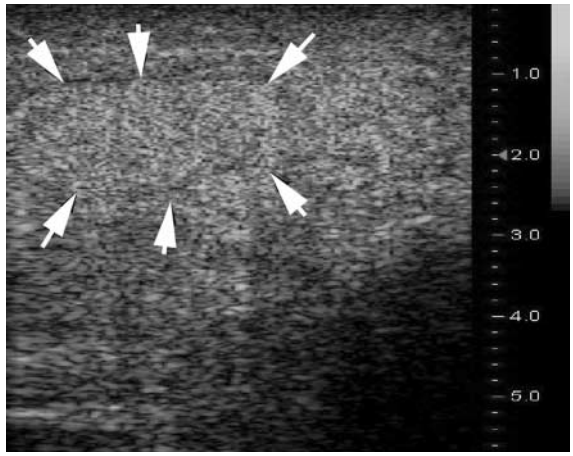

No scatterer size images were obtained for this patient, but of interest is the isoechoic nature of the lesion on the B-mode image. At this imaging frequency, no remarkable differences exist between the normal parenchyma and the nodule. It is unknown whether a change in imaging frequency or a parametric image of scatterer size might provide improved image contrast. However, relative echogenicity is often used without regard to the imaging protocol and hardware used to acquire the images, including no knowledge of the exact frequency setting on the machine. In fact, these factors can have a drastic impact on the appearance of lesions, depending on the acoustic properties of the tissue being imaged.

Figure 3B is a longitudinal B-mode image of another solitary nodule, this one having a hypoechoic appearance compared with the normal thyroid parenchyma depicted immediately to the left. The elastogram and the scatterer size image (averaged over the first 20 planes) corresponding to this nodule are in Figure 3, A and C, respectively. Considerable contrast of the lesion versus the background tissue is observed in both parametric images. The nodule appears to have smaller scatterers and exhibits less strain on compression than the adjacent parenchyma, where the scatterer radius is shown in the color bar. The elastogram appears to have more distinct margins that correspond to those on the B-mode image compared with those in the scatterer size image. The mild enhancement seen on the B-mode image is likely the cause of the scatterer size shadowing just beyond the nodule because this would have caused an overestimation of the backscatter coefficient in this area. However, the contrast in the nodule versus the adjacent parenchyma is still quite observable on the scatterer size image.

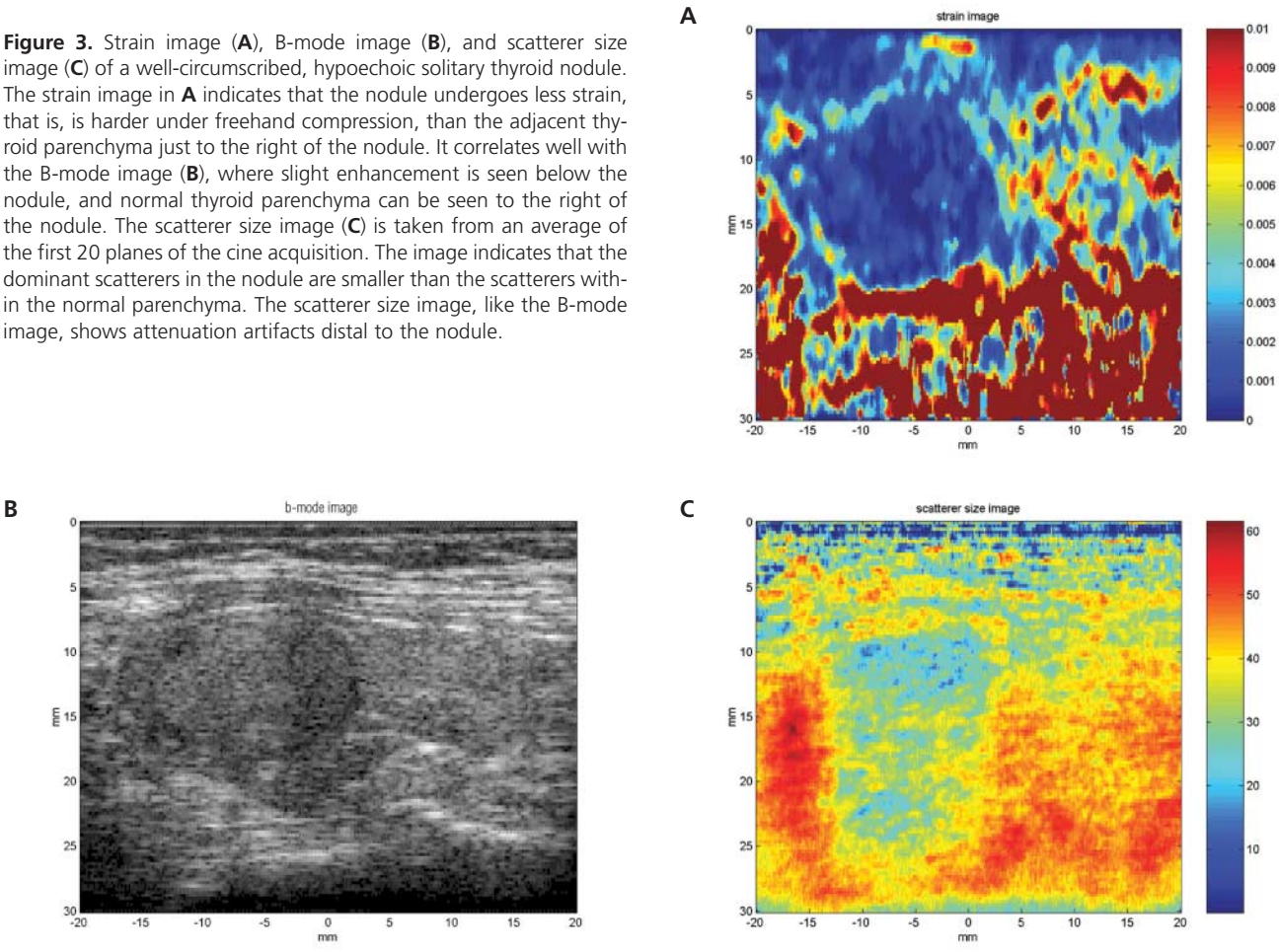

Figure 3. Strain image (**A**), B-mode image (**B**), and scatterer size image (**C**) of a well-circumscribed, hypoechoic solitary thyroid nodule. The strain image in **A** indicates that the nodule undergoes less strain, that is, is harder under freehand compression, than the adjacent thyroid parenchyma just to the right of the nodule. It correlates well with the B-mode image (**B**), where slight enhancement is seen below the nodule, and normal thyroid parenchyma can be seen to the right of the nodule. The scatterer size image (**C**) is taken from an average of the first 20 planes of the cine acquisition. The image indicates that the dominant scatterers in the nodule are smaller than the scatterers within the normal parenchyma. The scatterer size image, like the B-mode image, shows attenuation artifacts distal to the nodule.

Another example is presented in Figure 4. Unlike in the previous case, pathologic findings were available and indicated that this patient had Hurthle cell carcinoma. Figure 4B is a transverse B-mode image of 2 nodules in the right lobe of the thyroid; corresponding elastogram and scatterer size images are in Figure 4, A and C, respectively. The strain image indicates that the nodules have less strain, that is, are harder under freehand compression, than the adjacent parenchyma. The scatterer size image (averaged over the first 5 planes) shows less remarkable contrast compared with that seen in Figure 3 but still appears to have smaller scatterers than tissue seen immediately above and to the right of the nodules.

Table 1 presents a summary of results on patients undergoing thyroid scanning to date. Results show there appears to be considerable contrast observed between nodules and thyroid parenchymal tissue for both types of parametric images. This suggests that further work to determine the diagnostic importance of these parameters in characterizing thyroid nodules is worthwhile.

Discussion

As reported by a number of researchers, relative echogenicity is currently either viewed as not being statistically significant or at best a common but weak predictor of malignancy in B-mode sonography of the thyroid.[14–16] Although it may be true that relative echogenicity is not a sensitive test to differentiate cancer at the frequency range currently used in these retrospective studies, it is not clear whether standardization of machine settings has been implemented in a way that would ensure that such results are universally applicable. It is also possible that some of the variations among researchers may be due to other factors such as user and machine differences. For example, as

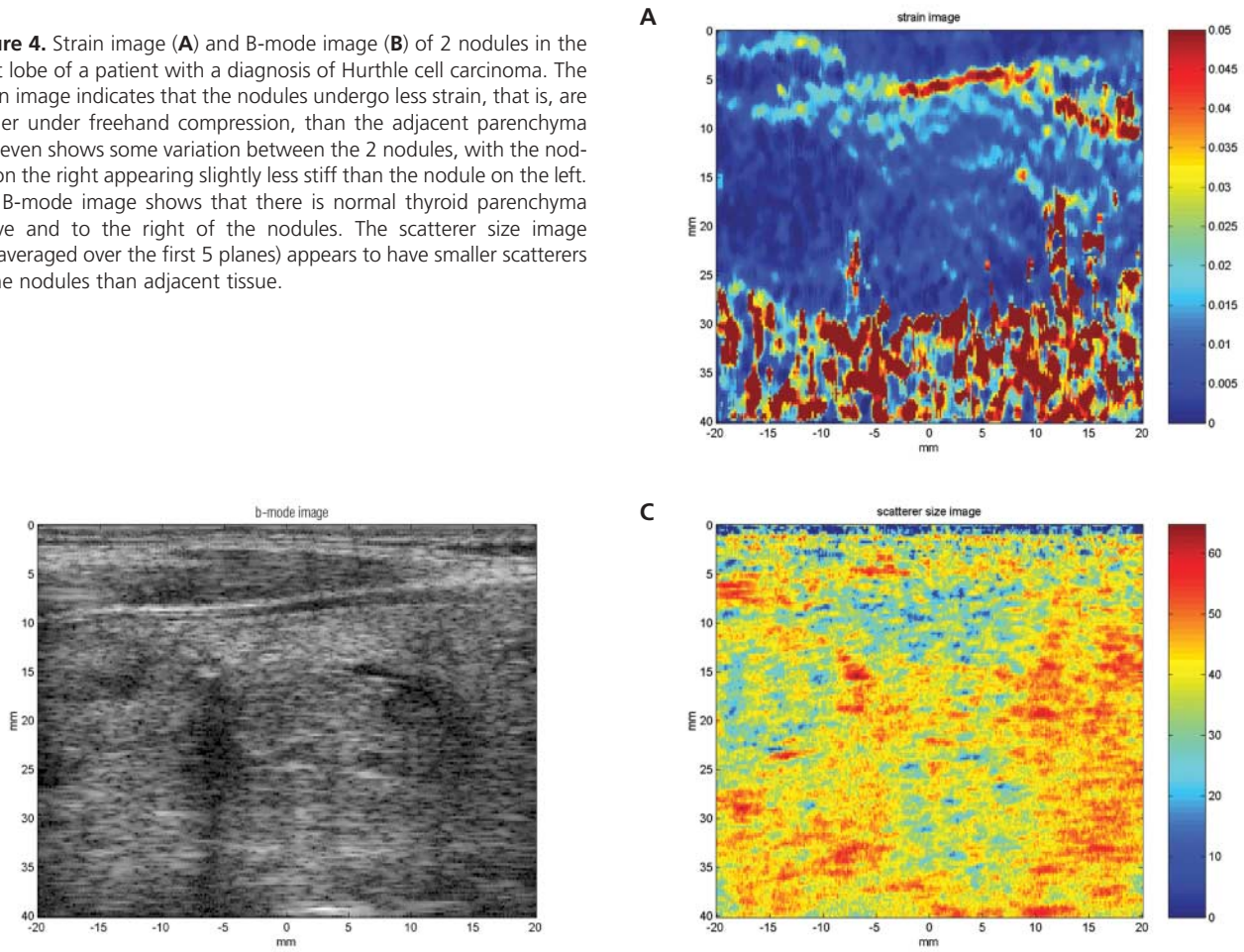

Figure 4. Strain image (**A**) and B-mode image (**B**) of 2 nodules in the right lobe of a patient with a diagnosis of Hurthle cell carcinoma. The strain image indicates that the nodules undergo less strain, that is, are harder under freehand compression, than the adjacent parenchyma and even shows some variation between the 2 nodules, with the nodule on the right appearing slightly less stiff than the nodule on the left. The B-mode image shows that there is normal thyroid parenchyma above and to the right of the nodules. The scatterer size image (**C**) (averaged over the first 5 planes) appears to have smaller scatterers in the nodules than adjacent tissue.

shown by Wilson et al,[17] the effective imaging frequency of a scanner can vary measurably with modest adjustments in the controls of the machine, such as transmit focal depth. Such changes in effective imaging frequency and bandwidth are not generally reported to the operator. However, any appreciable variations in backscatter and attenuation, which are frequency dependent, between thyroid nodules and normal tissue may have a considerable impact on the viewed relative brightness on B-mode images. This was shown clinically in a report by Sommer et al,[18] in which changes in contrast-noise ratios of relatively high- versus low-frequency sonographic images were observed when imaging liver tumors. Also, tissue harmonic imaging was shown by Szopinski et al[19] to improve lesion detectability in thyroids with the use of a comparison of relative gray scale levels of the nodule versus adjacent parenchyma.

One parameter that may play an important role in explaining these phenomena is the size of dominant scatterers at the frequency range used by the ultrasound machine. This is one reason why the results presented in this work are of interest. Contrast was observed between thyroid nodules and normal parenchyma with the use of scatterer size estimates, and unlike relative B-mode echogenicity, this difference is based on an objective estimate, which strives to eliminate system dependencies. The estimates are still limited by the bandwidth of the transducer and system but are not limited to the postprocessing involved in the formation of B-mode (amplitude-only) images. Gross differences on hematoxylin-eosin–stained histologic specimens of benign and cancerous thyroid disease can be easily observed at both the architectural and cellular levels.[20] Whether these differences contribute to a diagnostically relevant difference on effective scatterer size images is yet to be determined, but if proven to be the case, it might notably contribute to the treatment of patients in the future. It should be noted that we used a gaussian autocorrelation model in computing scatterer sizes. To be effective, this requires a frequency bandwidth that presents a *ka* value greater than or equal to 0.5 and less than or equal to 1.6 (where k is the wave number, $2\pi/\lambda$, λ being the wavelength and a the effective scatterer radius).[21] This is slightly different than the bandwidth requirements of 0.5 and 1.2 found by Insana and Hall[22] and Insana et al[23] using Faran's scattering theory.[24] The required bandwidth for such a measurement is depicted in black in Figure 5 for different scatterer sizes. This discussion is included to show that the current system may be a reasonable one for imaging thyroid structures given their typical sizes under histo-

Table 1. Results for Thyroid Imaging of Scatterer Size and Strain

	Contrast		
Parametric Mode	**+**	**0**	**–**
Scatterer Size*	4	5	4
Relative Strain†	4‡	2	3

Qualitative comparison of contrast observed within a patient group of 13 and a normal group of 4 was performed. A positive (+) contrast in size indicates an observed larger effective scatterer size versus normal parenchyma, and a + contrast for the relative strain indicates a softer (greater percent strain) structure than adjacent tissue. Negative (–) indicates a smaller diameter or harder structure. Some of the patients had a diffuse condition rather than a nodule or simply no nodule present. Therefore, strain data were only given for 9 patients.

*Size contrast was determined by the observed contrast between the normal and abnormal tissue, and when considering diffuse conditions, comparison was made with the values obtained for the normal group of 4 subjects.

†Strain contrast was only estimated if abnormal and normal tissue was captured in the same palpation.

‡A fibroadenoma acquired previously using a Terason scanner was included as having a greater percent strain than the surrounding thyroid tissue.

Figure 5. Required bandwidth (black) to yield an accurate estimation of the spatial autocorrelation function used in determining the effective scatterer size for effective scatterer diameters from 20 to 200 μm.

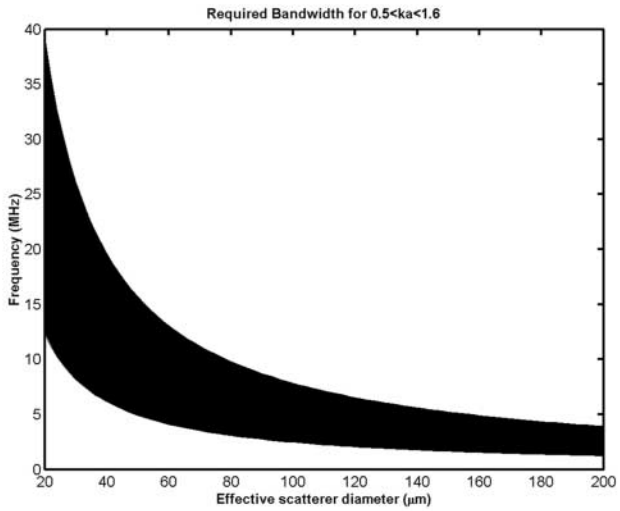

logic staining; that is, normal thyroid follicles are around 100 to 200 μm in diameter. In looking at our initial results, our size ranges are from around 20 to 200 μm. Although the accuracy of these determinations will eventually require close comparison with histopathologic findings and greater knowledge of the actual sources of scattering, we can refer to Gerig et al,[25] who have analyzed the accuracy of scatterer size determinations for dominant scatterers in phantoms. They reported SDs on the order of the estimated scatterer size for small scatterers, 51 μm, and around 10% for large scatterers, 232 μm. It should be noted that they used a 3.35-MHz array with an approximate bandwidth of 70%, which, given Figure 5 as a selection criterion, was inappropriate to cover the full range of sizes accurately in their phantom. They also reported the ability to reduce the larger deviation by about 50% by exploiting spatial angular compounding, which increased the number of "uncorrelated" estimates used in backscatter calculations. Obviously, further investigation of the sources of dominant scattering in thyroid and thyroid cancers at these particular bandwidths is needed. However, given the observed contrast presented here, such studies are warranted. The thyroid remains a very good candidate for this type of imaging because current sonography systems provide broad-bandwidth transducers capable of imaging at sufficiently high frequencies to allow accurate estimates of the size ranges reported here. Spatial compounding should further improve our estimates. In addition, to better understand these new sonographic applications in the thyroid, we would suggest formulating phantoms with characteristics similar to those of the thyroid for optimization of algorithms and the use of animal studies to accurately identify sources of scattering in thyroid.

The preliminary results presented in this article indicate that contrast can be observed between thyroid nodules and adjacent parenchyma with the use of 2 quantitative parameters, estimates of the dominant effective scatterer size and relative differences in strain. No correlation to pathologic findings is presented at this time, but the differences observed are promising. These new imaging modes hold out the prospect of improving differentiation of thyroid nodules in vivo and thus ideally removing the need for more invasive procedures such as FNA. If FNAs are not eliminated, they still stand to be improved by better guidance of needles to suggestive sites. All of this, of course, will be dependent on refinement of the images, determination of the relevance of these parameters in classifying tissue, and realization of these modes in real time. It is not known whether quantitative images can supplant or supplement current B-mode and color flow imaging studies in the classification of thyroid nodules, but given the observed differences reported here, further studies are warranted. Continued work in the optimization of these modes is ongoing.

References

1. US Preventive Services Task Force. Guide to Clinical Preventive Services. 2nd ed. Washington, DC: US Department of Health and Human Services, Office of Disease Prevention and Health Promotion; 1996.
2. Muro-Cacho C, Ku N. Tumors and tumor-like lesions of the thyroid gland. In: Pellitteri P, McCaffrey T (eds). Endocrine Surgery of the Head and Neck. San Diego, CA: Singular Publishing Group, Inc; 2002:21–47.
3. Solbiati L, Charboneau J, James EM, et al. The thyroid gland. In: Rumack CM, Wilson SR, Charboneau JW (eds). Diagnostic Ultrasound. 2nd ed. St Louis: Mosby-Year Book; 1998:703–729.
4. Castro M, Gharib H. Thyroid nodules and cancer: when to wait and watch and when to refer. Postgrad Med 2000; 107:113–124.
5. Insana MF, Wood JG, Hall TJ. Identifying acoustic scattering sources in normal renal parenchyma in vivo by varying arterial and ureteral pressures. Ultrasound Med Biol 1992; 18:587–599.
6. Lizzi FL, Ostromogilsky M, Feleppa EJ, et al. Relationship of ultrasonic spectral parameters to features of tissue microstructure. IEEE Trans Ultrason Ferroelectr Freq Control 1987; 3:319–329.
7. Lyshchik A, Higashi T, Asato R, et al. Elastic moduli of thyroid tissues under compression. Ultrason Imaging 2005; 27:101–110.
8. Hall TJ, Zhu Y, Spalding CS. In vivo real-time freehand palpation imaging. Ultrasound Med Biol 2003; 29:427–435.
9. Garra BS, Cespedes EI, Ophir J, et al. Elastography of breast lesions: initial clinical results. Radiology 1997; 202:79–86.
10. Gerig A, Zagzebski J, Varghese T. Statistics of ultrasonic scatterer size estimation with a reference phantom. J Acoust Soc Am 2003; 113:3430–3437.
11. Yao LX, Zagzebski JA, Madsen EL. Backscatter coefficient measurements using a reference phantom to extract depth-dependent instrumentation factors. Ultrason Imaging 1990; 12:58–70.
12. Fujii Y, Taniguchi N, Itoh K, Omoto K. Attenuation coefficient measurement in the thyroid. J Ultrasound Med 2003; 22:1067–1073.

13. Varghese T, Techavipoo U, Liu W, et al. Elastographic measurement of area and volume of thermal lesions resulting from radiofrequency ablation. AJR Am J Roentgenol 2003; 181:701–707.

14. Kim EK, Park CS, Chung WY, et al. New sonographic criteria for recommending fine-needle aspiration biopsy of nonpalpable solid nodules of the thyroid. AJR Am J Roentgenol 2002; 178:687–691.

15. Iannuccilli J, Cronan J, Monchik J. Risk for malignancy of thyroid nodules as assessed by sonographic criteria. J Ultrasound Med 2004; 23:1455–1464.

16. Papini E, Guglielmi R, Bianchini A, et al. Risk of malignancy in nonpalpable thyroid nodules: predictive value of ultrasound and color-Doppler features. J Clin Endocrinol Metab 2002; 87:1941–1946.

17. Wilson TA, Zagzebski J, Li Y. A test phantom for estimating changes in effective frequency of an ultrasound scanner. J Ultrasound Med 2002; 21:937–945.

18. Sommer G, Olcott EW, Tai L. Liver tumors: utility of characterization at dual-frequency US. Radiology 1999; 211:629–636.

19. Szopinski KT, Wysocki M, Pajk AM, Slapa RZ, Jakubowski W, Szopinska M. Tissue harmonic imaging of thyroid nodules. J Ultrasound Med 2003; 22:5–12.

20. Corsaro A, Lazzaro C, Sloffer C. Pathology Education Resources Laboratory (PERL). Indianapolis, IN: Indiana University School of Medicine; 1998.

21. Dong F. Characterizing Tissue Microstructure Using an Ultrasound System-Independent Spatial Autocorrelation Function [PhD dissertation]. Madison, WI: University of Wisconsin; 1999.

22. Insana MF, Hall TJ. Parametric ultrasound imaging from backscatter coefficient measurements: image formation and interpretation. Ultrason Imaging 1990; 12:245–267.

23. Insana MF, Wagner RF, Brown DG, Hall TJ. Describing small-scale structure in random media using pulse-echo ultrasound. J Acoust Soc Am 1990; 87:179–192.

24. Faran JJ. Sound Scattering by Solid Cylinders and Spheres. Cambridge, MA: Harvard University; 1951. Technical memorandum 22.

25. Gerig AL, Varghese T, Zagzebski JA. Improved parametric imaging of scatterer size estimates using angular compounding. IEEE Trans Ultrason Ferroelectr Freq Control 2004; 51:708–715.